Thermochimica Acta 515 (2011) 24–31

Contents lists available at ScienceDirect

Thermochimica Acta

journal homepage: www.elsevier.com/locate/tca

Study on thermal decomposition of calix[4]arene and its application in thermal stability of polypropylene

K. Chennakesavulu*, M. Raviathul Basariya, P. Sreedevi, G. Bhaskar Raju, S. Prabhakar, S. Subba Rao

National Metallurgical Laboratory Madras Centre, CSIR Complex, Taramani, Chennai 600113, India

ARTICLE INFO

Article history:
Received 25 June 2010
Received in revised form
10 November 2010
Accepted 16 December 2010
Available online 29 December 2010

Keywords:
Calix[4]arene
Thermal decomposition
Activation energy
Friedman analysis
Model-fitting methods

ABSTRACT

Thermal decomposition kinetics of calix[4]arene (C4) was investigated using thermogravimetric analysis (TGA) and derivative of TG curve (DTG). TG experiments were carried out under static air atmosphere with nominal heating rates of 1.0, 2.5, 5.0 and 10.0 K/min. Model-fitting methods and model-free methods such as Friedman and Ozawa–Flynn–Wall methods were employed to evaluate the kinetic parameters such as activation energy (E_a), exponential factor ($\ln A$) and reaction order (n). To determine the antioxidant property of C4 the non-isothermal kinetics of polypropylene (PP) with C4 as additive was studied. The FTIR, ESR and ^{13}C NMR CP-MAS techniques were used to propose the decomposition mechanism of C4 in the presence of PP.

1. Introduction

Calixarenes are cyclic oligomers (general formulae: $C_{7n}H_{6n}O_n$) which are derived by the condensation of phenol–formaldehyde in alkali media and are capable of forming complexes with metal ions, anions and neutral molecules [1]. It is reported that in USA alone, nearly 20,000 tonnes of antioxidants were consumed during 1983 for the stabilization of plastics, it clearly reveals the importance of antioxidants in polymer industry [2]. In last two decades, high molecular weight calix[n]arenes have been of major industrial interest because of their low mobility in polymeric materials like polyolefins. It is also reported that calix[n]arenes are inhibitors of polyolefins auto-oxidation [3]. The antioxidant activity of the calixarenes was studied by chemiluminescence methods in thermal stabililization of polyethylenes and this proves that the calixarenes are good antioxidant additives for polyethylenes [4]. Feng et al. reported that the thermal stability effect of p-tert-butylcalix[n]arene on γ-radiation degradation of polypropylene was due to the suppression of PP chain scission by calix[n]arene [5]. The thermal stability of the calixarenes needs to be established due to the higher melting points of calix[n]arene and lack of experimental data concerning polyolefins-calixarene additive systems. Though the inclusion behavior of calixarenes with different solvents [6,7] was studied with TGA at different atmospheres, to the best of our knowledge this is the first thermo-kinetic study reported on thermal degradation of C4. In the present study the evaluated kinetic parameters of C4 suggests its applicability as an antioxidant for PP.

2. Experimental

2.1. Materials

The analytical grade chemicals p-tert-butyl phenol, polypropylene, formaldehyde, para-formaldehyde, $AlCl_3$ and HPLC grade solvents such as chloroform, toluene, xylene and methanol were purchased from Merk speciality chemicals. HPLC grade solvents are used as received without further purification.

2.2. Synthesis of calix[4]arene

5, 11, 17, 23-Tetra-t-butyl-35, 36, 37, 38-tetra hydroxy calix[4]arene was synthesized as earlier reported [8]. The obtained p-tert-butyl calix[4]arene was further de-tert-butylated with $AlCl_3$/toluene as described in the literature to obtain 25, 26, 27, 28-tetrahydroxycalix[4]arene [9].

* Corresponding author at: National Metallurgical Laboratory Madras Centre, CSIR Complex, Taramani, Chennai, Tamil Nadu 600113, India. Tel.: +91 44 2254 2077; fax: +91 44 2254 1027.
E-mail addresses: chennanml@yahoo.com, chenna_velpumadugu@yahoo.com (K. Chennakesavulu).

0040-6031/$ – see front matter © 2010 Elsevier B.V. All rights reserved.
doi:10.1016/j.tca.2010.12.012

2.3. Characterization of 25, 26, 27, 28-Tetrahydroxycalix[4]arene (C4)

Melting point: 587–589 K; LCMS-ESI $(M-1)^+$: 423; elemental analysis: molecular formulae $C_{28}H_{24}O_4$, calculated (C, 79.22%), (H, 5.70%), found (C, 78.87%), (H, 5.12%); ^{1}H NMR (500 MHz, pyridine-d5) δ (ppm): 9.7 (s, 4H, –OH), 7.1 (d, 8H, Ar–H), 6.6 (t, 4H, Ar–H), 4.1 (bs, 8H, Ar–CH_2–); ^{13}C NMR (500 MHz, pyridine-d5) δ (ppm): 150.3, 129.1, 121.4, 116, 31.7; DEPT-NMR (500 MHz, pyridine-d5) δ (ppm): 149.9, 129.1, 121.4, 116 (aromatic ring –CH), 31.7 (bridged methylene –CH_2–); ^{13}C NMR CP-MAS (300 MHz, pyridine-d5) δ (ppm): 151.6, 129, 122, 120, 31.6.

2.4. Characterization

^{1}H NMR, ^{13}C NMR and DEPT-NMR were obtained by using Bruker Avance-500 MHz NMR spectrometer. Solid state ^{13}C NMR cross polarisation magic angle spinning spectrum (^{13}C NMR CP-MAS) was obtained by using Bruker Avance 300 MHz NMR spectrometer. The samples were taken in 2.5 mm diameter of zircon rotors and spun at 7 kHz. The elemental analysis was done with Euro Vectors Elemental analyzer. HPLC and LCMS-ESI analysis were done with Schimadzu and Agilent instruments respectively. X-band ESR spectra was recorded on a Bruker-EMX spectrometer, at room temperature with a modulation frequency of 100 kHz and microwave power set at 3.2 mW. The g values were measured by taking DPPH as an external reference. The error in the reported g values is of the order of 0.0002. The FTIR spectrum of C4 and thermally treated C4 samples are recorded at room temperature by Perkin Elmer Instrument.

2.5. Sample preparation

Generally calix[n]arene forms stable inclusion complexes with volatile organic guest molecules. In order to remove the traces of solvents in C4 cavity, prior to the TGA experiments the sample was degassed at 473 K under vacuum (10^{-5} Torr) for 48 h. The mixture of polypropylene and C4 are taken in an agate bowl and ground well with agate pestle results. High specific surface area of the calixarenes will facilitate to contact with maximum amount of polypropylene [10].

2.6. Thermogravimetric analysis

TGA/DTG experiments were performed with Versa Therm Cahn thermo balance TG-151 with sensitivity of 10 μg. Thermal experiments were conducted in the temperature range of 300–1100 K with samples weighing around 20 ± 0.01 mg. The analyses were carried out at four nominal heating rates (1.0, 2.5, 5.0 and 10.0 K/min) under static air atmosphere. Generally, the efficiency of antioxidants in polymers is determined by three processes: the chemical reactivity, physical loss and a minimal effective concentration [11]. The physical loss of antioxidants may enhance under flowing nitrogen or any other atmosphere. In order to reduce the physical loss (evaporation, leaching and blooming) of antioxidant the static air atmosphere was preferred in the present study. DTA was carried out using Netzsch 409C model with 5.0 K/min heating rate. The Netzsch thermo kinetics software was used for the kinetic analysis of experimental data.

2.7. Theoretical background

The kinetic analysis of solid state thermal decomposition [12,13] was governed by a single step kinetic equation (1).

$$\frac{d\alpha}{dt} = k(T)f(\alpha) \tag{1}$$

where α is the conversion of the reaction, $d\alpha/dt$ is the Rate of conversion, $f(\alpha)$ is the reaction model and $k(T)$ is the temperature dependent rate constant

The fractional conversion α is expressed as $(m_0 - m_t)/(m_0 - m_f)$, where m_0 and m_f are the initial and final weights of the sample, respectively, and m_t is the weight of the sample at time t. The explicit temperature dependence of the rate constant is described according to the Arrhenius equation (2).

$$k(T) = A\exp\left(-\frac{E_a}{RT}\right) \tag{2}$$

By combining Eqs. (1) and (2) the following is obtained.

$$\frac{d\alpha}{dt} = A\exp\left(\frac{-E_a}{RT}\right)f(\alpha) \tag{3}$$

where A is the pre-exponential factor (rate constant at infinite temperature), R is the gas constant, E_a is the apparent activation energy and T is the absolute temperature.

According to non-isothermal kinetic theory, the fractional conversion α can be expressed as a function of temperature, which is dependent on the time of heating. The explicit time dependence of Eq. (3) can be eliminated through the trivial transformation

$$\frac{d\alpha}{dT} = \frac{1}{\beta}A\exp\left(\frac{-E_a}{RT}\right)f(\alpha) \tag{4}$$

where $\beta = dT/dt$ is the heating rate

Kinetic parameter calculations based on TGA data can be obtained from Eqs. (3) and (4). In the present study, two different approaches namely model-free methods [14–16] and model-fitting methods [17] were used to calculate the kinetic parameters. The kinetic parameters obtained using non-isothermal data was observed to be advantageous over conventional isothermal studies [18].

2.7.1. Model-free or isoconversional method

To gain more information regarding the decomposition mechanism, model-free methods which are recommended as a trustworthy were adopted for kinetic analysis. The basic assumption of these methods is that the reaction model is independent of the heating rate [19].

The E_a values calculated by this method are independent of any implicit reaction model, which allows one to explore multi step kinetics [20,21]. The most common model-free methods such as Friedman [14] and Ozawa–Flynn–Wall [15,16] were employed for the thermo-kinetic analysis of C4 and PP.

2.7.1.1. Friedman method. The method [22] based on the inter comparison of the rate of conversion $d\alpha/dt$ for a given degree of conversion α determined using dynamic heating rate β is considered as the most general derivative technique.

After taking logarithms of Eq. (4) and rearranging, we obtain

$$\ln\left(\beta\frac{d\alpha}{dT}\right) = \ln[Af(\alpha)] - \frac{E_a}{RT} \tag{5}$$

The E_a values over a wide range of conversions were obtained by plotting $\ln(\beta\, d\alpha/dT)$ versus $1/T$ for a constant α value.

2.7.1.2. Ozawa–Flynn–Wall method. This method [15,16] is an integral method which can determine the E_a without the knowledge of reaction order for given values of conversion.

Table 1
Algebraic expression for $f(\alpha)$ and $g(\alpha)$ for the various kinetic reaction models.

S.No.	Reaction model	Code	$f(\alpha)$	$g(\alpha)$
1	First order	F1	$1-\alpha$	$-\ln(1-\alpha)$
2	Second order	F2	$(1-\alpha)^2$	$(1-\alpha)^{-1}-1$
3	Third order	F3	$(1-\alpha)^3$	$0.5(1-\alpha)^{-2}-1$
4	Avrami Erofeev equation	A2	$2(1-\alpha)[-\ln(1-\alpha)]^{1/2}$	$[-\ln(1-\alpha)]^{1/2}$
5	Avrami Erofeev equation	A3	$3(1-\alpha)[-\ln(1-\alpha)]^{2/3}$	$[-\ln(1-\alpha)]^{1/3}$
6	Avrami Erofeev equation	A*n*	$n(1-\alpha)[-\ln(1-\alpha)]^{(1-1/n)}$	$[-\ln(1-\alpha)]^{1/n}$
7	Prout–Tomkins equation	B1	$\alpha(1-\alpha)$	$\ln[\alpha/(1-\alpha)]$
8	1D diffusion	D1	$1/2\alpha$	α^2
9	2D diffusion	D2	$[-\ln(1-\alpha)]^{-1}$	$\alpha+(1-\alpha)\ln(1-\alpha)$
10	Jander's equation	D3	$(3/2)(1-\alpha)^{2/3}[1-(1-\alpha)^{1/3}]^{-1}$	$[1-(1-\alpha)^{1/3}]^2$
11	Ginstling–Brounstein	D4	$(3/2)[(1-\alpha)^{-1/3}-1]^{-1}$	$1-2\alpha/3-(1-\alpha)^{2/3}$
12	2D phase boundary	R2	$2(1-\alpha)^{1/2}$	$1-(1-\alpha)^{1/2}$
13	3D phase boundary	R3	$3(1-\alpha)^{2/3}$	$1-(1-\alpha)^{1/3}$

Integrating Eq. (4) and rearranging, we obtain

$$\log\beta = \log\frac{AE_a}{g(\alpha)R} - 2.314 - \frac{0.4567E_a}{RT} \quad (6)$$

where

$$g(\alpha) = \int_0^{\alpha}\frac{d\alpha}{f(\alpha)} \quad (7)$$

By plotting $\log\beta$ against $1/T$ at certain conversion rate, the slope $-E_a/R$ leads to E_a.

2.7.2. Model-fitting method

The model-fitting kinetic analysis depends on the reaction type and reaction model. The reaction models used for analysis include one to six step processes, in which the individual steps are linked as independent, competing and parallel reactions. Each model with selected reaction types gives quite reliable and consistent kinetic parameters. The reaction model may take various forms based on nucleation and nucleus growth, phase boundary reaction, diffusion and chemical reaction [22–24]. The unknown parameters were found from the fitting of measured data with the simulated curves for the given model and reaction types. The different kinetic reaction models [12,13] used for the analysis to identify the best one are represented in Table 1.

3. Results and discussion

3.1. Thermal decomposition of C4

The TGA/DTG curve of C4 is shown in Fig. 1a. The thermal decomposition of C4 occurred in the range of temperature 600–950 K with a total mass loss of 98%. It is interesting to note that C4 follows the two stage decomposition. The first stage decomposition occurred in the range of 600–750 K with mass loss of 40%. At this stage (i.e. 750 K) the samples are quenched and subjected for various instrumental techniques to determine the degradation of pathway for C4.

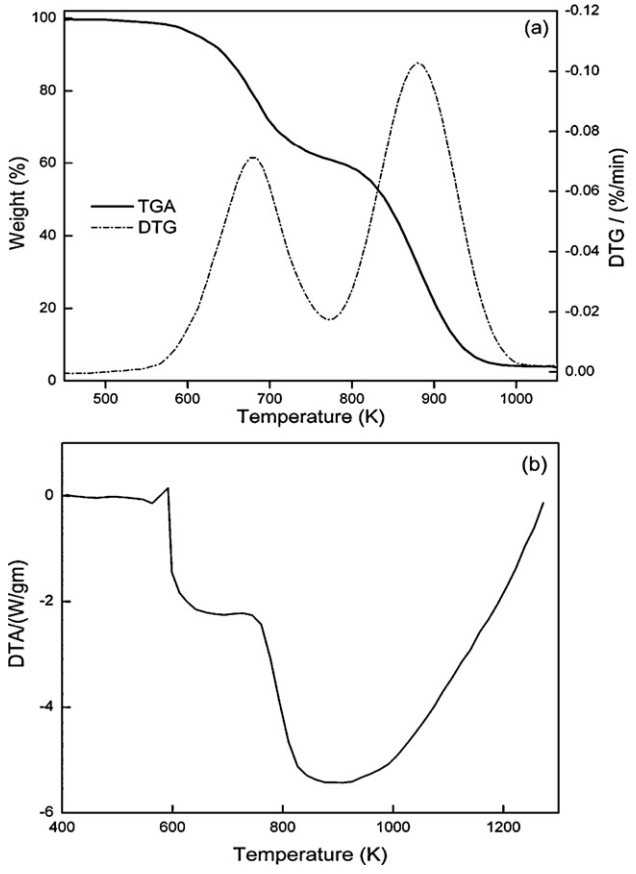

Fig. 1. (a) TGA/DTG curves C4 (heating rate: 10.0 K/min) and (b) DTA curve of C4 (heating rate: 5.0 K/min, here upward peaks corresponds to endothermic peaks).

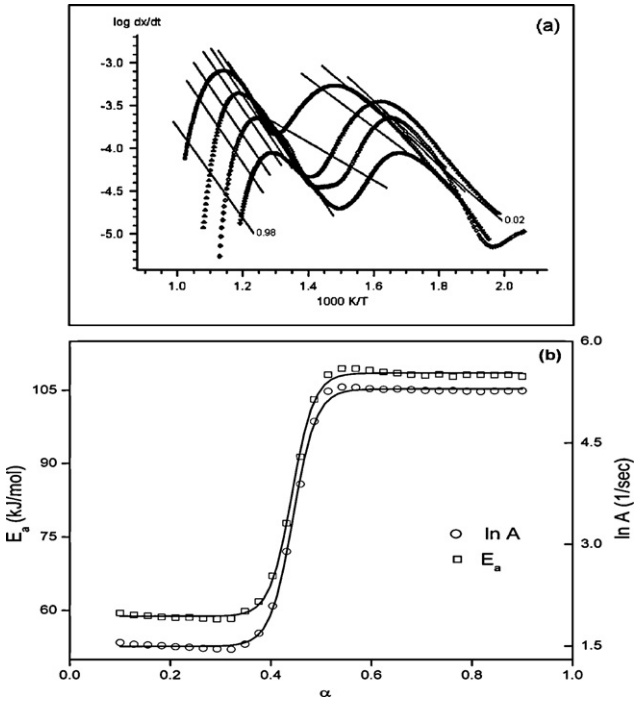

Fig. 2. (a) Friedman analysis of C4 (heating rates: 1.0, 2.5, 5.0 and 10.0 K/min). (b) E_a vs. α plot (here the ln A values are evaluated by using F1 kinetic model).

Table 2
Kinetic triplets of C4 for $A \rightarrow B \rightarrow C$ reaction model with non-linear regression.

Model $A \rightarrow B$	E_{a1} (kJ/mol)	$\ln A_1$ (1/s)	Model $B \rightarrow C$	E_{a2} (kJ/mol)	$\ln A_2$ (1/s)	r^2
F1	67	2.2	F1	119	3.9	0.9954
F1	62	1.7	D1	108	4.8	0.9999
F2	106	6.1	F2	197	10.2	0.9916
F*n*	97	5.2	F*n*	112	4.1	0.9906
A2	41	0.3	A2	54	0.2	0.9012
A3	25	1.1	A3	29	1.5	0.8965
A*n*	30	0.6	A*n*	23	1.1	0.9013
B_{na}	288	23	B_{na}	187	9.0	0.9236
D1	105	5.8	D1	105	3.4	0.9998
D2	119	6.9	D2	113	3.7	0.9975
D3	141	8.3	D3	135	4.6	0.9983
D4	127	7.0	D4	119	3.5	0.9983
R2	78	3.2	R2	94	2.6	0.9983
R3	80	3.3	R3	97	2.6	0.9984

The second stage decomposition occurred in the range of 750–950 K with mass loss of 45%. The loss of inclusioned methanol molecules in C4 [25] is not seen in the present case as the sample was degassed prior to TGA. The DTA curve of C4 is shown in Fig. 1b. An endothermic peak was observed around 590 K indicating the melting of the C4 and an endothermic peak between 700 K and 850 K indicates the cleavage of methylene group from phenolic arene groups.

3.2. The kinetics of decomposition of C4

The Friedman analysis for the thermal decomposition reaction of C4 and its corresponding energy plots is shown in Fig. 2. These plots show good separation of the two consecutive reactions i.e. $A \rightarrow B \rightarrow C$ with some scatter of points at the beginning and end of the plots. As the thermal decomposition proceeds, the E_a remains constant and reaches a maximum value for at α 0.3–0.6. This increase in E_a implies the depolymerisation reaction and results the open chain polyphenols. Usually, the methylene bridge between two phenolic rings is very stable. The phenolic –OH activates the breakage of methylene linkage (depolymerisation reaction) due to keto-enol tautomerism [26]. On further decomposition E_a remains constant. Thus it can be concluded that the E_{a1} of the first reaction step is lower than that of the E_{a2}. The differential Friedman E_a plot leads to apparent E_{a1} of 60 kJ/mol, E_{a2} of 110 kJ/mol and $\ln A_1$ of 1.5/s, $\ln A_1$ of 5/s respectively. In case of model-fitting approach the non-linear regression models were used for the calculation of kinetic parameters. The most probable kinetic model was analyzed by choosing best fit based on the value of the correlation coefficient (r^2) which was close to one. The E_a, $\ln A$ and r^2 for non-linear regression methods of C4 are shown in Table 2. Among the tested models, the C4 obeyed the reaction model $A \xrightarrow{F1} B \xrightarrow{D1} C$. Fig. 3 shows the fitted curves for non-linear regression of the TGA kinetic data for a two step degradation of C4. It can be concluded that the calculated E_a values from model-free and model-fitting methods were close to each other. Therefore, the determined kinetic triplets are reasonable and can be applied to arrive at the best kinetic models for C4.

3.3. ESR analysis

The ESR spectra of TGA quenched solid calix[4]arene at 745 K are shown in Fig. 4. The ESR spectrum shows a symmetrical singlet, this might probably due to the formation of isotropic free radicals. The *g* factor was measured to be 2.0045. The g-value is depends on the orientation of crystal and radical situated in a crystal with respect to applied magnetic field. The free radicals of water soluble calix[*n*]arenes do not show their hyperfine interaction, as the formed radical is in the centre of –OH groups of calix[*n*]arenes cavity [27]. The quenched sample was kept unanalyzed for one week, but the ESR signal still appeared, proving the stability of the formed free radicals.

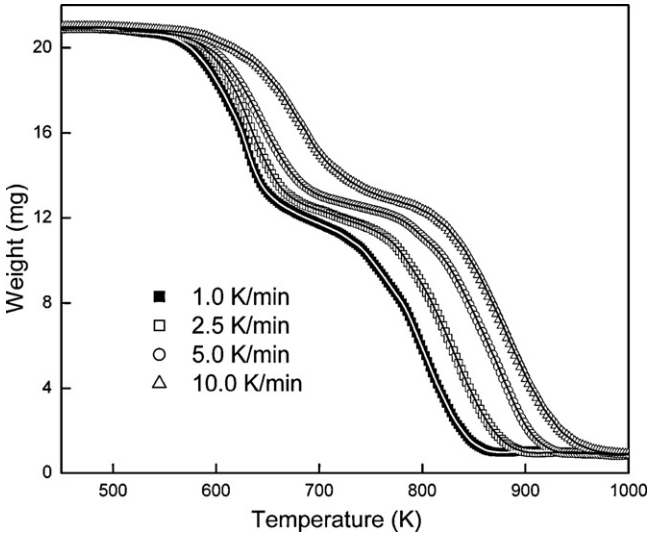

Fig. 3. Fit of TG measurements of C4, simulated with reaction model. $A \xrightarrow{F1} B \xrightarrow{D1} C$ (here $r^2 = 0.9999$).

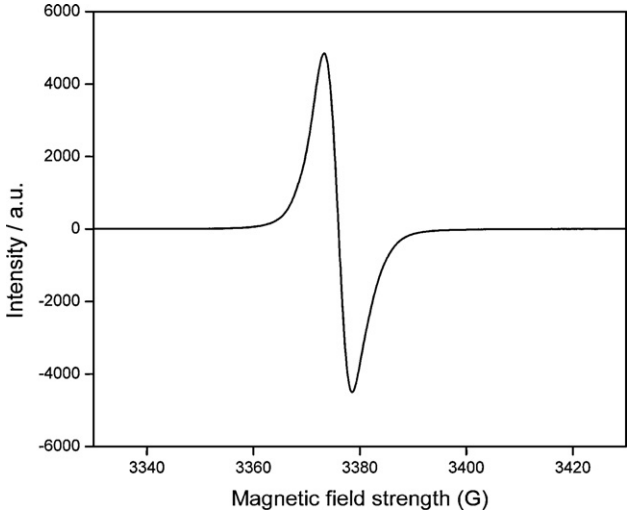

Fig. 4. ESR spectrum of TC4 at 745 K.

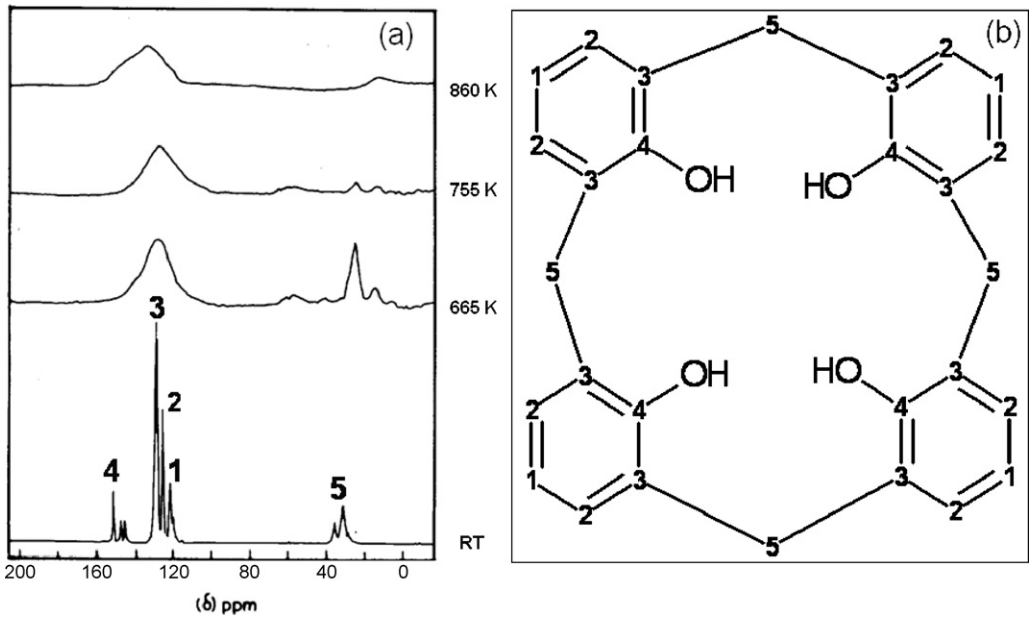

Fig. 5. ^{13}C NMR CP-MASS of TC4 at various temperatures.

3.4. ^{13}C NMR CP-MAS analysis

The ^{13}C NMR CP-MAS of C4 at room temperature and quenched samples at various temperatures are shown in Fig. 5. It appears that at room temperature, the aromatic carbons (1–4, which are numbered in Fig. 5b) are observed from 151 ppm to 120 ppm whereas signals corresponding to bridged methylene carbons (5 in Fig. 5b) are observed at 31 ppm. The signals corresponding to aromatic carbons at various temperatures was found to broaden drastically in the case of quenched calix[4]arene. The broadened aromatic carbon signal obtained may be due to the formation of stable phenoxy free radical and delocalization of free electron throughout the arene ring. Similar broader signals were observed by Qin et al. due to the formation of free radicals within the apocynum fiber in its ^{13}C NMR CP-MAS [28]. Finally the bridged methylene signal was shifted and almost disappeared at 860 K. This indicates the environment of the saturated carbon was modified with the temperature and thus the formation of new species from C4.

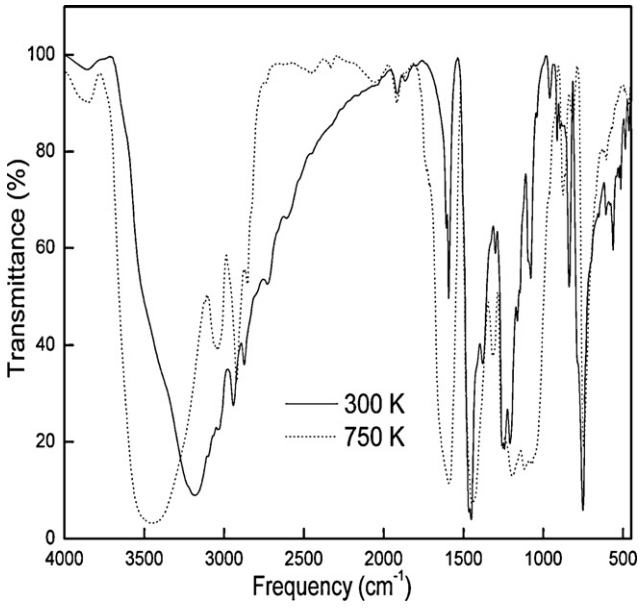

Fig. 6. FTIR analysis of C4.

3.5. FTIR analysis

The FTIR of C4, thermally treated C4 (TC4) quenched at 750 K during TG measurement are recorded at room temperature and shown in Fig. 6. All the observed bands of C4 are well matches with the literature elsewhere [29–31]. The bands at 3541, 3232 and 3152 cm^{-1} refers to –OH stretching vibration of C4. This indicates the strong hydrogen bond of rigid C4. In the case of TC4, the phenolic broad band shifts to 3434 cm^{-1} indicating the presence of free phenolic groups (i.e. open chain poly phenols formed from C4 which is free from strong hydrogen bonding). The C4 bands at 2933 and 2868 cm^{-1} corresponds to asymmetric and symmetric –CH stretching of methylene groups respectively. But in TC4 the corresponding –CH stretching vibration bands are shifted to 2921 and 2853 cm^{-1} respectively. This clearly suggests the breakage of C4 cavity at bridged methylene with phenolic groups. The bands of C4 at 1607 and 1593 cm^{-1} corresponds to aromatic ring –C=C– stretching vibrations. In the case of TC4 these bands appears as a high intensity broad singlet 1580 cm^{-1}. This indicates formation of C–O· in C4 cavity [32]. The band of C4 at 1440–1470 cm^{-1} corresponds to vibrations of aromatic –C=C–H and $-CH_2-$ bending vibrations. In the case of TC4, the corresponding bands are appeared

Table 3
Kinetic triplets of PP for various reaction models.

Model	E_a (kJ/mol)	ln A (1/s)	r^2
F1	175	12.2	0.9980
F2	157	10.2	0.9999
F*n*	158	10.4	0.9999 (*n* = 2.0)
A2	135	7.8	0.9920
A3	137	8.0	0.9847
A*n*	184	11.6	0.9913 (*n* = 0.7)
B_{na}	174	11.0	0.9823 (*n* = 1.0)
D1	182	11.1	0.9951
D2	194	11.9	0.9960
D3	213	12.9	0.9968
D4	200	11.7	0.9908
R2	145	8.2	0.9867
R3	147	8.2	0.9874

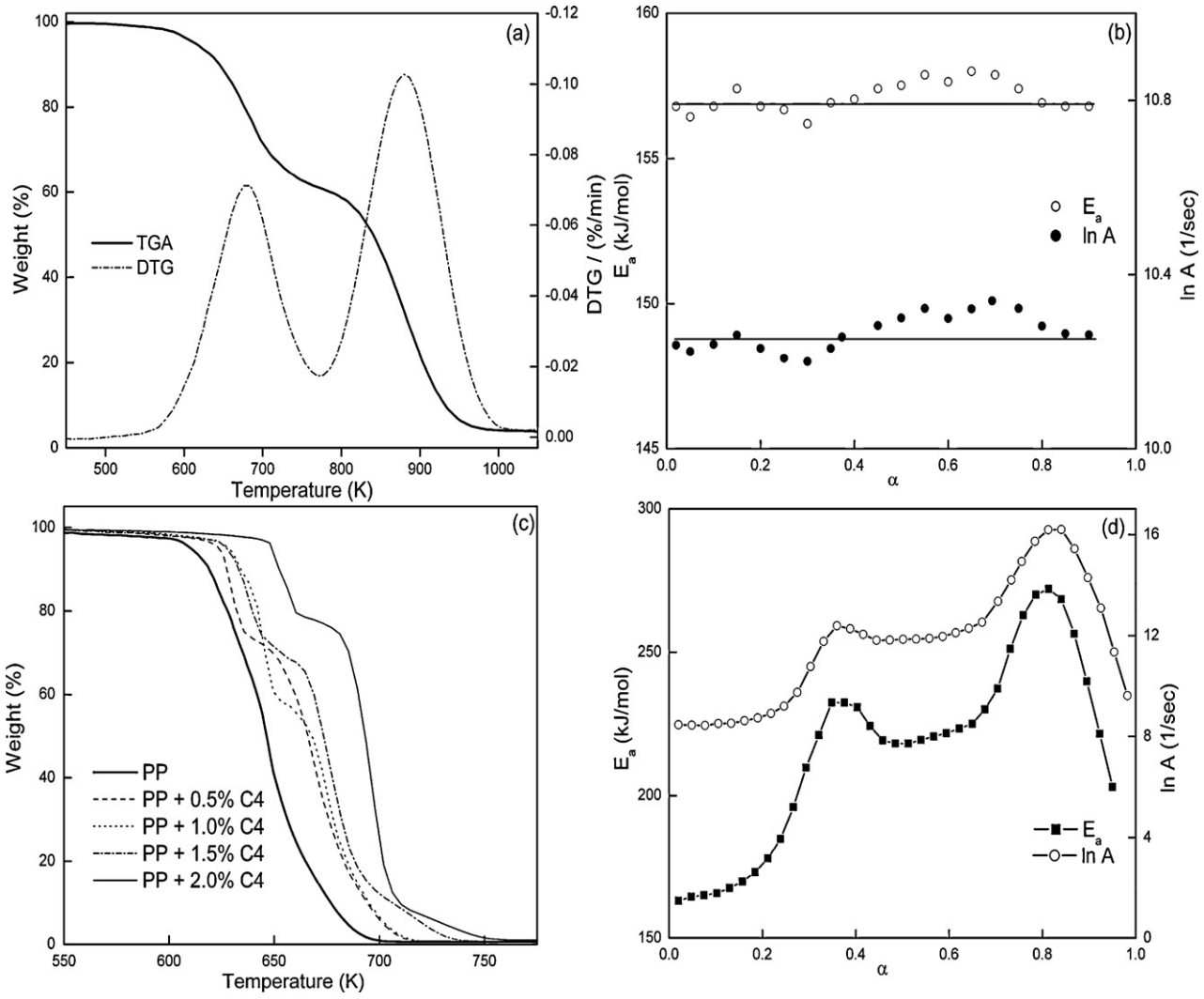

Fig. 7. (a) TGA/DTG of polypropylene (heating rate: 1.0 K/min). (b) Friedman E_a plot of PP. (c) TGA of PP + C4. (d) Friedman Ea plot of PP + 2% C4.

as a broad band around 1450 cm^{-1}. This indicates the aromatic ring vibration was obscured by $-CH_2-$ vibration [33]. The band of C4 at 1250 cm^{-1} refers asymmetric stretch of C–C–OH stretching vibration. In the case of TC4 the corresponding band was observed at 1190 cm^{-1} indicates the formation of C–O species. At RT the high intensity bands of C4 at 838 and 750 cm^{-1} corresponds to –C–H out of plane bending vibrations. In the case of TC4 the corresponding bands are shifted to 812 and 736 cm^{-1} respectively. This confirms the formation of ortho and para substituted benzene products.

3.6. Thermal decomposition kinetics of PP with C4

The TGA/DTG of PP at 1.0 K/min is shown in Fig. 7a. It shows that the degradation of polypropylene occurs in a single step in the temperature range of 600–900 K. In order to obtain the kinetic triplets of PP and PP + 2% C4 the non-isothermal TGA measurements were done at 1.0, 2.5, 5.0 and 10.0 K/min. From Fig. 7b the calculated E_a and ln A of PP from Friedman analysis were 158 kJ/mol and 10.3/s respectively, whereas Ozawa–Flynn–Wall analysis results in 160 kJ/mol of E_a and 10.5/s of ln A. The corresponding kinetic parameters of PP through model-fitting method are shown in Table 3. Aboulkas et al. reported that the E_a of 207 kJ/mol, ln A of 31/s and first order for decomposition of PP under nitrogen environment [34]. Peterson et al. reported that the E_a of ≈200 kJ/mol and ≈90 kJ/mol for nitrogen atmosphere and air atmosphere respectively [35]. The effect of atmospheric oxygen was the reason for variation of E_a. The free radicals generated during thermal decomposition can react with oxygen and results propagation reaction with newly oxidized free radicals formation may cause the lowering of E_a values. In present study, based on the correlation coefficient the decomposition of PP obeys the F2 reaction model. TGA of PP was done in the presence of various weight percentages of C4, the results are presented in Fig. 7c. Thermo oxidative degradation of PP was reduced with increase in C4 weight percentage. The critical stabilizer concentration of C4 was yet to be determined for thermo oxidative degradation of PP. In the presence of C4, the single step TG curve of PP becomes multi step decomposition. It is evident that during decomposition of PP, the C4 is exhibiting its antioxidant activity. Generally, the efficiency of antioxidant capacity depends on the effect induced by the phenolic groups, the spatial protections of double bond by delocalization of π-electrons and the interaction of oxygen atoms of OH units and the trapped radicals [5]. The non-isothermal kinetic analysis of PP + 2.0% of C4 mixture was done based on the TGA data collected at heating rates of 1.0, 2.5, 5.0 and 10.0 K/min. The high density polyethylene and low density polyethylenes can be thermally stabilized by the addition of 0.2–1.0% of calix[n]arenes [4]. Friedman E_a plots of PP and PP + 2.0% C4 mixture are shown in Fig. 7b and d. The E_a plot of PP + 2.0%

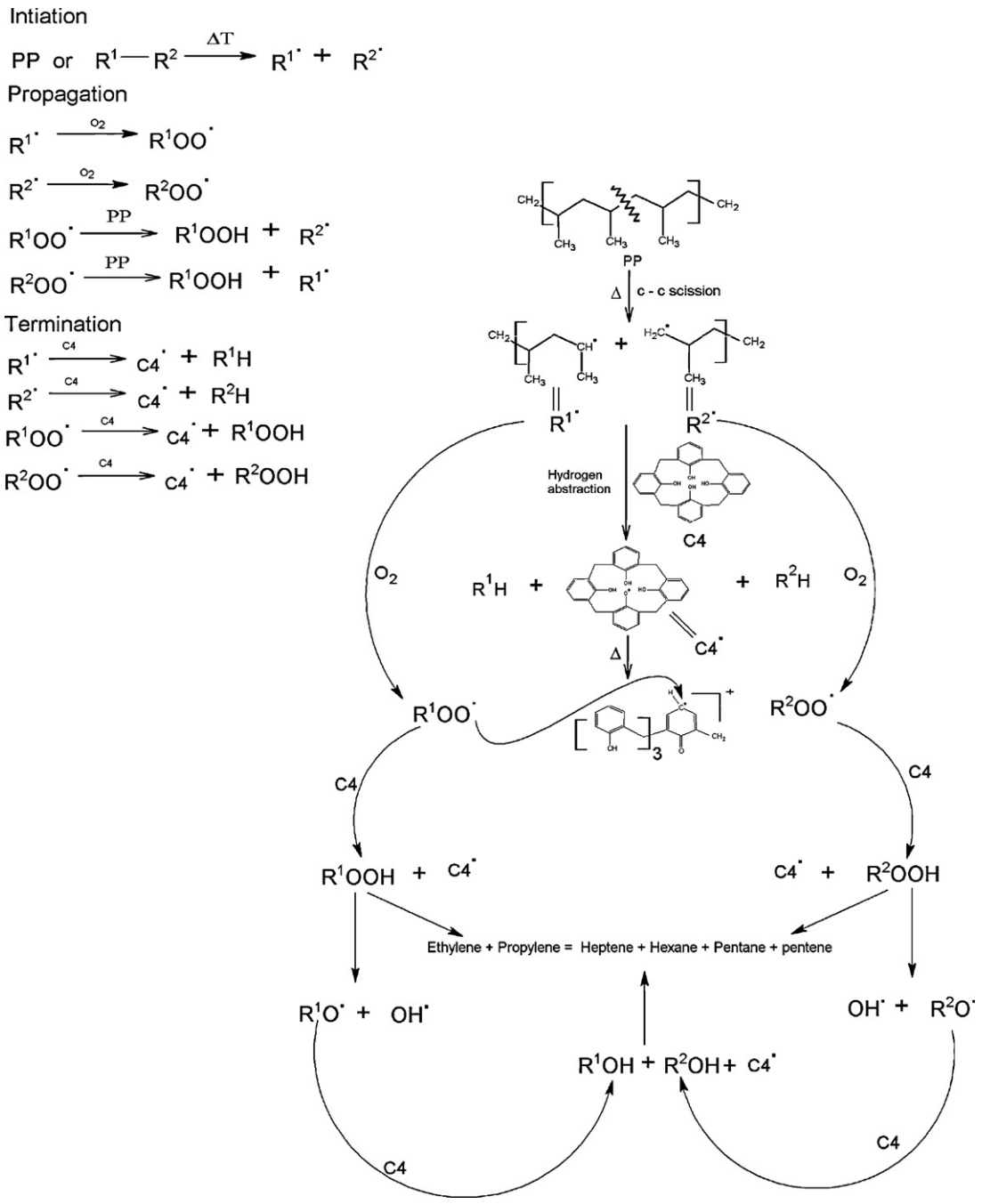

Fig. 8. Antioxidant activity of C4 during thermal decomposition of PP.

C4 reveals the decomposition follows complex reactions. The E_a values were enhanced drastically due to the formation of stable intermediate during decomposition. From ESR, ^{13}C NMR CP-MAS, FTIR characterizations and the kinetic studies the decomposition mechanism of C4 in the presence of PP was proposed and is shown in Fig. 8. The pure PP was subjected to thermal decomposition, the initiation step involves the random C–C scission and results the formation of less stable primary and secondary radicals. In the presence of air atmosphere the propagation step involves the formation of peroxyradicals. In termination step the radicals may gain hydrogen atom from phenolic groups of C4 and form paraffins or olefins. At higher temperatures the formed C4 free radicals result the open chain polyphenolic free radicals. Thus the presence of C4 prevents the decomposition of PP. The FTIR and ESR analysis confirms the formation of stable open chain polyphenolic free radicals.

4. Conclusions

Thermal decomposition of C4 obeys the two step decomposition mechanism $A \xrightarrow{F1} B \xrightarrow{D1} C$. During the decomposition of C4 the formation of stable open chain polyphenolic free radicals were confirmed by FTIR, ^{13}C NMR CP-MAS and ESR techniques. The C4 was examined as an additive for thermal decomposition of PP and its kinetic parameters are also evaluated. The decomposition of PP follows the single step decomposition (F2 reaction model), but in the presence of a 0.2–2.0% of C4 the PP obeys the multi step decompo-

sition. The decomposition mechanism of C4 in the presence of PP was proposed. The TGA experiments and Friedman E_a plots of PP and PP + 2.0% C4 clearly shows the antioxidant property of C4.

Acknowledgements

The authors K. Chennakesavulu and M. Raviathul Basariya Senior Research Fellows are grateful to Council of Scientific and Industrial Research (CSIR), New Delhi (India) for the financial support. The authors are grateful to NMR Facility, SAIF-Indian Institute of Technology, Madras (India) and NMR Centre-Indian Institute of Science, Bangalore (India) for providing the necessary spectral and analytical data.

Appendix A. Supplementary data

Supplementary data associated with this article can be found, in the online version, at doi:10.1016/j.tca.2010.12.012.

References

[1] C.D. Gutsche, Calixarenes, in: Monographs in Supramolecular Chemistry, Royal Society of Chemistry, London, UK, 1989.
[2] J. Pospisil, Polym. Degrad. Stabil. 20 (1988) 181–202.
[3] K. Seiffarth, M. Schulz, G. Gormar, J. Bachmann, Polym. Degrad. Stabil. 24 (1989) 73–80.
[4] S. Jipa, T. Zaharescu, R. Setnescu, M. Dumitru, L.M. Gorghiu, I. Mihalcea, M. Bumbac, Polym. Degrad. Stabil. 80 (2003) 203–208.
[5] W. Feng, L.H. Yuan, S.Y. Zheng, G.L. Huang, J.L. Qiao, Y. Zhou, Radiat. Phys. Chem. 57 (2000) 425–429.
[6] M. Lazzarotto, F.F. Nachtigall, E. Schnitzler, E.E. Castellano, Thermochim. Acta 429 (2005) 111–117.
[7] J. Schatz, F. Schildbach, A. Lentz, S. Rastatter, J. Chem. Soc., Perkin Trans. 2 (1998) 75–77.
[8] C.D. Gutsche, B. Dhawan, K.H. No, R. Muthukrishnan, J. Am. Chem. Soc. 103 (1981) 3782–3792.
[9] C.D. Gutsche, L.G. Lin, Tetrahedron 42 (1986) 1633–1640.
[10] K. Chennakesavulu, G. Bhaskar Raju, S. Prabhakar, J. Phys. Org. Chem. 23 (2010) 723–729.
[11] A. Boersma, Polym. Degrad. Stabil. 91 (2006) 472–478.
[12] M.E. Brown, D. Dollimore, A.K. Galwey, Reactions in the Solid State Comprehensive Chemical Kinetics, vol. 22, Elsevier, Amsterdam, 1980.
[13] J. Sestak, Thermophysical Properties of Solids Comprehensive Analytical Chemistry, vol. 12D, Elsevier, Amsterdam, 1984.
[14] H. Friedman, J. Polym. Sci. 6C (1963) 183–195.
[15] T. Ozawa, Bull. Chem. Soc. Jpn. 38 (1965) 1881–1886.
[16] J.H. Flynn, L.A. Wall, J. Res. Natl. Bur. Stand. Sect. A—Phys. Chem. 70A (1966) 487–493.
[17] S. Vyazovkin, C.A. Wight, Thermochim. Acta 340–341 (1999) 53–68.
[18] Q.P. Hu, X.G. Cui, Z.H. Yang, J. Therm. Anal. 48 (1997) 1374–1379.
[19] S. Vyazovkin, J. Comput. Chem. 18 (1997) 393–402.
[20] S. Vyazovkin, Int. J. Chem. Kinet. 28 (1996) 95–101.
[21] S. Vyazovkin, N. Sbirrazzuoli, Macromol. Rapid. Commun. 27 (2006) 1515–1532.
[22] S. Vyazovkin, C.A. Wight, Chem. Mater. 11 (1999) 3386–3393.
[23] S. Vyazovkin, Thermochim. Acta 355 (2000) 155–163.
[24] J.T. Sun, Y.D. Huang, G.F. Gong, H.L. Cao, Polym. Degrad. Stabil. 91 (2006) 339–346.
[25] H. Deligoz, O. Ozen, G.K. Cilgi, H. Cetisli, Thermochim. Acta 426 (2005) 33–38.
[26] D.W. Van Krevelen, Chimia 28 (1974) 504–517.
[27] A. Tanaka, H. Yashiro, A. Ishigaki, H. Murai, Appl. Magn. Reson. 37 (2010) 581–593.
[28] Z. Qin, Z. Xin, Z. Jian-Bing, T. Jun, F. Zhao-Tian, S. Wan-Fu, Nucl. Sci. Technol. 17 (2006) 38–42.
[29] V.L. Furer, E.I. Borisoglebskaya, V.I. Kovalenko, Spectrochim. Acta Part A 61 (2005) 355–359.
[30] P. Opaprakasit, A. Scaroni, P. Painter, J. Mol. Struct. 570 (2001) 25–35.
[31] A. Amiri, F. Babaeie, M. Monajjemi, Phys. Chem. Liq. 46 (2008) 379–389.
[32] A.I. Brodskii, L.A. Kotorienko, S.A. Samoilenko, V.D. Pokhodenko, J. Appl. Spectrosc. 14 (1971) 633–638.
[33] I. Poljansek, M. Krajnc, Acta Chim. Slov. 52 (2005) 238–244.
[34] A. Aboulkas, K. El Harfi, A. El Bouadili, M. Ben Chanda, A. Mokhlisse, J. Therm. Anal. Calorim. 89 (2007) 203–209.
[35] J.D. Peterson, S. Vyazovkin, C.A. Wight, Macromol. Chem. Phys. 202 (2001) 775–784.